Agriculture, Ecosystems and Environment 375 (2024) 109197

Contents lists available at ScienceDirect

Agriculture, Ecosystems and Environment

journal homepage: www.elsevier.com/locate/agee

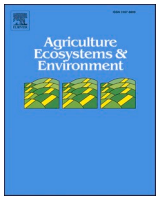

Can mineral soil coverage be a suitable option to mitigate greenhouse gas emissions from agriculturally managed peatlands?

Sonja Paul [a,*,1], Christof Ammann [a], Yuqiao Wang [a], Christine Alewell [b], Jens Leifeld [a,b]

[a] Climate and Agriculture Group, Agroscope, Reckenholzstrasse 191, Zürich 8046, Switzerland
[b] Environmental Sciences, University of Basel, Bernoullistrasse 30, Basel CH-4056, Switzerland

ARTICLE INFO

Keywords:
Organic soil
Drained peatland
Greenhouse gas emissions
Mineral soil cover
Mitigation measure
Eddy covariance

ABSTRACT

The agricultural use of organic soils usually requires drainage, resulting in soil subsidence and high greenhouse gas (GHG) emissions, mainly CO_2. One proposed strategy to maintain the productivity of these soils is adding a mineral soil cover. However, its impact on the GHG budget has yet to be discovered. Herein, we determined the net ecosystem carbon budget (NECB) for a pair of covered (Cov) and uncovered (reference, Ref) organic soils under intensive grassland management in the Rhine Valley, Switzerland, over four years (1 March 2018–1 March 2022). The net ecosystem exchange (NEE) of CO_2 was measured using the eddy covariance method, in addition to recording carbon exports and imports by harvest and organic fertilisers. N_2O and CH_4 fluxes were measured using an automatic time-integrating chamber system over three years. Both of the drained peatlands under agricultural use showed substantial soil organic carbon (SOC) losses of 175–786 g C m^{-2} $year^{-1}$ (Ref) and 125–826 g C m^{-2} $year^{-1}$ (Cov). The annual losses were driven by the aerated peat carbon stock during summer and accounted for 0.5 – 1.4 % of it. Covering the organic soil with a mineral layer did not significantly reduce the SOC losses relative to the reference site in any of the four years, and CH_4 uptake was marginal. However, soil coverage significantly reduced the three-year average N_2O emissions from 1.5 (Ref) to 0.2 g N m^{-2} $year^{-1}$ (Cov) and consequently the net GHG budget from 19.2±2.0 to 12.8±2.1 t CO_2 eq. ha^{-1} $year^{-1}$. We conclude that mineral soil coverage *per se* has little potential to reduce SOC losses from drained organic soils. However, if combined with a considerable rise in the water table, SOC losses may be effectively reduced while maintaining agricultural productivity.

1. Introduction

The steady accumulation of soil organic matter in peatlands due to slow microbial decomposition under water-saturated conditions has led to an essential global soil organic carbon (SOC) store. During the Holocene, about 600 Pg of SOC accumulated in the corresponding organic soils, equivalent to ~20 % of the global soil organic carbon stock, despite covering a small global surface area of only 3 % (Yu et al., 2010; Leifeld and Menichetti, 2018). Peatlands are also an essential pool of organic nitrogen soil containing 8–15 Gt N (Leifeld and Menichetti, 2018).

To provide aerobic conditions for crops not adapted to high groundwater tables (GWTs), a considerable portion of these wet soils was drained, leading to substantial soil subsidence owing to the physical processes and rapid mineralisation of the aerated peat (Erkens et al., 2016). These processes together result in long-term average soil subsidence rates of about 2 cm $year^{-1}$ for crop- and grasslands (Paul and Leifeld, 2023). Subsidence prevents the sustainable use of drained organic soils mainly for two reasons: first, peat mineralisation induces exceedingly high greenhouse gas (GHG) emissions, turning the former carbon sink into a strong GHG source. Worldwide, the cultivation of degraded peatland generates 32 % of cropland GHG emissions, although less than 1 % of cropland is located on these soils (Carlson et al., 2017). Second, with ongoing soil subsidence, the aerated rooting zone continuously decreases, and the organic soil becomes wet again when approaching the lowered GWT. In the temperate zone, repeated expensive drainage is necessary every 40–50 years (Ferré et al., 2019) until all the peat is mineralised, as its subsequent suitability for long-term agricultural use depends strongly on the properties of the underlying mineral material. In addition to these subsidence-induced

* Correspondence to: Climate and Agriculture Group, Agroscope, Zürich, Switzerland.
E-mail address: sonjamarit.paul@agroscope.admin.ch (S. Paul).
[1] ORCID-iD: 0000-0001-6903-7539

https://doi.org/10.1016/j.agee.2024.109197
Received 24 November 2023; Received in revised form 14 July 2024; Accepted 17 July 2024
Available online 24 July 2024

challenges, wet organic soils have a low load-bearing capacity, restricting the use of agricultural machines after heavy rainfall; consequently, management of these soils is constrained by meteorology.

Carbon dioxide (CO_2) is a major component of GHG emissions from drained organic soils, amounting to an average emission rate of 360–810 g C m^{-2} $year^{-1}$ in temperate grasslands (Hiraishi et al., 2014; Tiemeyer et al., 2020). Meta-studies revealed GWT as one crucial driving factor. However, land use history, nutrient availability and peat quality add to the observed variability in the response of CO_2 emissions to drainage at different sites (Evans et al., 2021; Tiemeyer et al., 2020; Couwenberg and Fritz, 2012). Nitrous oxide (N_2O) is the second most important GHG from drained peatlands, with average N_2O emissions in the order of 0.16–0.82 g N m^{-2} $year^{-1}$ in the temperate zone (Hiraishi et al., 2014; Leppelt et al., 2014; Linn and Doran, 1984; Wang et al., 2022). Drained organic soils emit little methane or may even be small CH_4 sinks because anoxic soil conditions—the prerequisite for methane production—are seldom present in drained organic soils (Wilson et al., 2016; Evans et al., 2021). In addition to GHG emissions, high peat mineralisation rates cause enhanced nutrient mobilisation, leading to the risk of water eutrophication (Kløve et al., 2017, Kløve et al., 2010; Prévost et al., 1999).

Mitigating GHG emissions from agricultural soils is highly relevant to achieving climate stabilisation (Leahy et al., 2020), and these soils are particularly relevant in this context, as they are GHG emission hotspots. Rewetting drained soils and restoring peatlands have already been identified as ways to reduce GHG emissions (Darusman et al., 2023) by moderating CO_2 emissions or even returning the systems to carbon sinks (Evans et al., 2021; Tiemeyer et al., 2020; Wilson et al., 2016). However, once organic soils are rewetted, conventional upland production is no longer possible with most plants. This trade-off between environmental goals and the need for agricultural production presents a barrier to implementing peatland restoration (Ferré et al., 2019). Thus, measures towards sustaining agricultural production, and simultaneously protecting the SOC stock and reducing GHG emissions, are urgently needed.

One proposed measure to counteract soil subsidence and increase the trafficability of organic soils and possibly reduce GHG emissions is the addition of mineral soil material to the organic topsoil (Blankenburg, 2015; Sognnes et al., 2006; Wang et al., 2022). A mineral material with a 20–40-cm thickness is added onto the organic topsoil. It is either mixed with the underlying peat layer or retained as a covering layer (blanket) atop the organic soil. Besides sand, moraine material, material from construction sites or clayey material from coastal regions is used as a soil amendment (Blankenburg, 2015; Sognnes et al., 2006; Ferré et al., 2019). In the case of an organic topsoil with an existing underlying sand layer, deep ploughing can also be used to generate alternating tilted bars of sand and peat (German mixed-layer; Schindler and Müller, 1999). The addition of mineral material alters the physical and hydraulic properties, resulting in improved manageability and, ultimately, an increased yield on subsided organic soils (Bambalov, 1999; Blankenburg, 2015; Schindler and Müller, 1999; Sognnes et al., 2006).

While the benefit from the farmers' viewpoint is obvious, the influence of mineral soil coverage on peat protection and GHG emissions is poorly studied, although a mineral soil amendment to organic soils was mentioned as early as 1889 (Zakharova et al., 2020). Organic soils covered or mixed with sand may emit a similar amount of CO_2 as those without amendments (Beyer, 2014; Tiemeyer et al., 2016). However, a systematic side-by-side comparison of GHG emissions from a covered and non-covered peatland at the field scale, which eliminates confounding factors, such as different site properties or study times, is still missing. While there are hints that N_2O emissions are reduced by covering the organic soil with a mineral soil layer (Wang et al., 2022; Wüst-Galley et al., 2023), a full GHG budget that includes all relevant GHGs (CO_2, CH_4, N_2O) of the drained organic soil with and without a mineral soil cover is missing, despite being essential to the evaluation of possible co-benefits or trade-offs of such a measure.

Here, we analyse the effect of a mineral soil cover on GHG emissions in an intensively used grassland on drained organic soil in the Rhine Valley, Switzerland. The study aims to (i) evaluate the impact of soil coverage on GHG emissions (CO_2, CH_4, N_2O), ii) identify the driving forces of these emissions and (iii) extend the data basis of default emissions factors from drained organic soils for the Swiss GHG inventory. We used the eddy covariance (EC) method to measure CO_2 fluxes over four consecutive years, and an automatic integrating chamber system for measuring N_2O and CH_4 fluxes over three years.

2. Methods

2.1. Study site

The study site (47°16'48", 7°31'06", 427 m NN) is located in Rüthi, Switzerland, on the former floodplain of the Rhine River. The first instance of drainage using ditches was before 1890 (https://map.geo.admin.ch), but the practice intensified in the 1970s, first with a subsoil drainage system consisting of drainage pipes at 14-m intervals, and the site was used as a pasture. Over the years, productivity progressively deteriorated as water saturated the topsoil for most of the season. Due to the resulting low bearing capacity, the pasture was converted into an intensively used meadow in 2013, and to improve the manageability of the grassland, one part of the site was covered with mineral soil material in 2006–2007. The cover material was residual mineral soil from a nearby construction site. It was residual mineral soil material that, otherwise, would have been brought to a landfill site. Therefore, no additional emissions due to material transport were generated. For further improvements, the northern part of the covered site was covered a second time in October 2018, and the grassland has been intensively managed since 2013, including mineral and slurry fertilisation and five to six cuts per year, and management of the non-covered and covered parts was identical. Dominant grass species include *Lolium perenne*, *Alopecurus pratensis*, *Festuca arundinacea, Festuca pratensis* and *Trifolium pratense.* To investigate the effect of mineral coverage, we studied the covered site (Cov) in comparison to the adjacent non-covered site, which was considered the reference (Ref; Fig. 1, further details see supplement).

The soil at the Ref site is characterised by a peat layer of a thickness greater than 10 m, with the upper 0.3 m being highly earthified, as

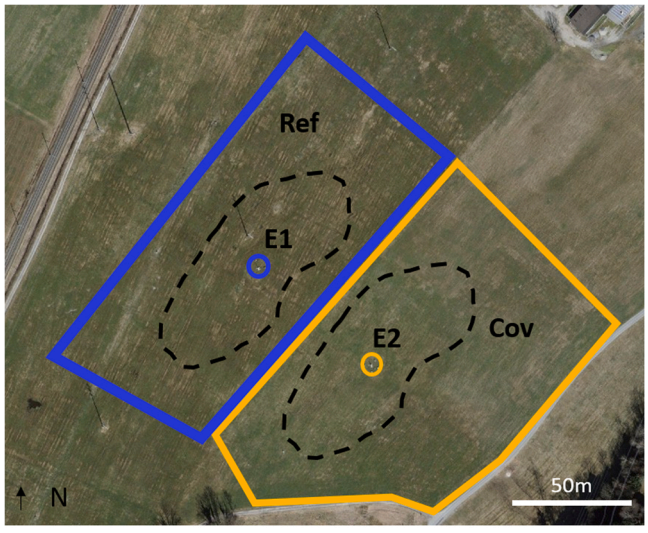

Fig. 1. Map of the study site Rüthi with two paired experimental sites without (Ref, blue framed area) and with (Cov, orange framed area) a mineral soil cover. Eddy covariance (EC) systems, groundwater observation wells, soil sensors and N_2O chambers were located at the centre of Ref (E1) und Cov (E2). Annual cumulative footprint contributions are indicated by the black dashed lines representing contributions of 80 %. Map: Image Swisstopo.

indicated by reduced SOC concentrations (17 %) and low C/N ratios (Fig. 2). This topsoil layer is underlain by sapric to fibric peat horizons with a SOC concentration of up to 48 %. The deeper horizons occasionally contain thin mineral interlayers of low carbon content. At Cov, the mineral coverage of the organic soil was 0.42 ± 0.08 m, containing 55 % silt, 29 % sand and 16 % clay (n = 12). The carbon stock of the peat layer of the first m was 54.2 ± 1.9 kg C m^{-2} and 46.9 ± 3.6 kg C m^{-2} (n = 12, mean ± 2SE) for Ref and Cov, respectively.

2.2. Components of the carbon budget

The net ecosystem carbon budget is the total rate of organic carbon accumulation (or loss) from ecosystems. Provided that the SOC loss due to erosion or leaching is negligible at the study site, biomass export by harvest ($F_{C\text{-}export}$), carbon import by slurry application ($F_{C\text{-}import}$) and gaseous carbon exchange as CO_2 (=NEE) and CH_4 ($F_{CH4\text{-}C}$) are the main processes determining the net ecosystem carbon budget (NECB), which can be expressed as follows (all terms in mass carbon per area and time):

$$-\frac{\Delta SOC}{\Delta t} = NECB = NEE + F_{CH4-C} + F_{C-export} - F_{C-import} \quad (1)$$

Eq. 1 follows the concept of Chapin et al. (2006). The system boundary is the soil/vegetation–atmosphere interface, where harvested biomass is counted as a loss from the system. Note that the gas exchange fluxes follow the micrometeorological sign convention, with positive values indicating an upward net flux (i.e., a carbon loss to the atmosphere), whereas negative values indicate a gain by the system (here, carbon input through organic fertiliser). On an annual or longer-term basis, the NECB is roughly equivalent to the change in SOC storage over time (ΔSOC/Δt). Gaseous CO_2 emissions, due to mineral weathering, represent a possible additional source of CO_2 not derived from peat mineralisation (Evans et al., 2016a). However, the contributions of calcareous minerals to organic horizons can be neglected due to the low pH. In contrast, the mineral cover contains calcareous minerals, but due to the high pH of the soil, only a minute amount is expected to emerge as CO_2 and thus contribute to overall GHG (Peacock et al., 2019). In addition, in most grassland systems, dissolved carbon losses to the aquifer are a minor component, with typical losses of dissolved organic carbon for temperate grasslands on organic soils in the order of 5–11 g C m^{-2} $year^{-1}$ (Evans et al., 2016a; Frank et al., 2017; Peacock et al., 2019), though carbon eroded from vegetated peat soils is negligible (Evans et al., 2019).

For the NECB calculation, all contributing quantities are expressed in terms of carbon mass, but to compare the radiative forcing of the different GHGs and for the analysis of the net GHG budget, annual fluxes are reported in units of CO_2 equivalents using the Intergovernmental Panel on Climate Change (IPCC) global warming potentials (GWPs) for GHG reporting and accounting (28 for CH_4 and 265 for N_2O relative to CO_2, and a time horizon of 100 years; Myhre et al., 2013). The net GHG budget (NGB) was calculated as follows (Soussana et al., 2010; Ammann et al., 2020):

$$NGB = \frac{44}{12}(NECB - F_{CH4-C}) + F_{CH4} \times GWP_{CH4} + F_{N2O} \times GWP_{N2O} \quad (2)$$

where methane flux has to be subtracted from NECB to prevent a partial double counting. The total uncertainty (95 % confidence interval, CI) of the NGB was calculated by combining the uncertainties of the individual components using Gaussian error propagation. The difference between Ref and Cov or between individual years was determined significant if the difference was smaller than its 95 % CI.

In this study, the annual budgets comprised the period March to March and were named Year 1 (1 March 2018–1 March 2019), Year 2 (1 March 2019–1 March 2020), Year 3 (1 March 2021– 1 March 2021) and Year 4 (1 March 2021–1 March 2022). Note that only the GHG budget of the grassland ecosystems is considered here. A full life cycle assessment of the mineral soil coverage measure was beyond the scope of this study.

2.3. Meteorological and soil measurements

Meteorological parameters were continuously monitored close to E2 (Fig. 1), whereas air temperature, pressure, relative humidity, global radiation and precipitation were measured using a Vaisala Weather Transmitter (WXT520, Finland). The device was mounted at the same height as the EC system (2.15 m above ground), and measurements were taken at 0.1 Hz, with average values recorded every 10 min on a CR1000 logger (Campbell Scientific, UK). Due to problems with the on-site precipitation measurement, the precipitation data shown in this study were taken from the MetoSwiss weather station in Sax, located about 7 km from our site.

For soil characterisation, 24 soil samples (0–1 m depth, 8 segments at 0.125 m in length and 0.05 m in diameter) were taken. Prior to the element analysis of C and N content (Hekatech, Germany), the samples were acidified. Nitrogen loss was estimated using the measured SOC loss and the assumption of a constant C/N ratio in the soil. Concerning pH, soil (10 g unground) was suspended in 0.01 M calcium chloride ($CaCl_2$), shaken at 160 cycles min^{-1} for 15 min and left overnight before the soil pH was measured with a flat surface electrode (pH3310, WTW, Germany). To determine the soil pore volume and pore diameter, 24 undisturbed cylindrical soil samples (100 cm^{-3}, from 0.03 to 0.08 m depth) were saturated from below and then drained to soil matric potentials of −30, −60, −100, −300 and −1500 kPa after Keller et al. (2019). Further, the water-filled pore space was calculated based on the difference between the volumetric water content (VWC) and total pore volume.

Soil water content and soil temperature were measured (using the

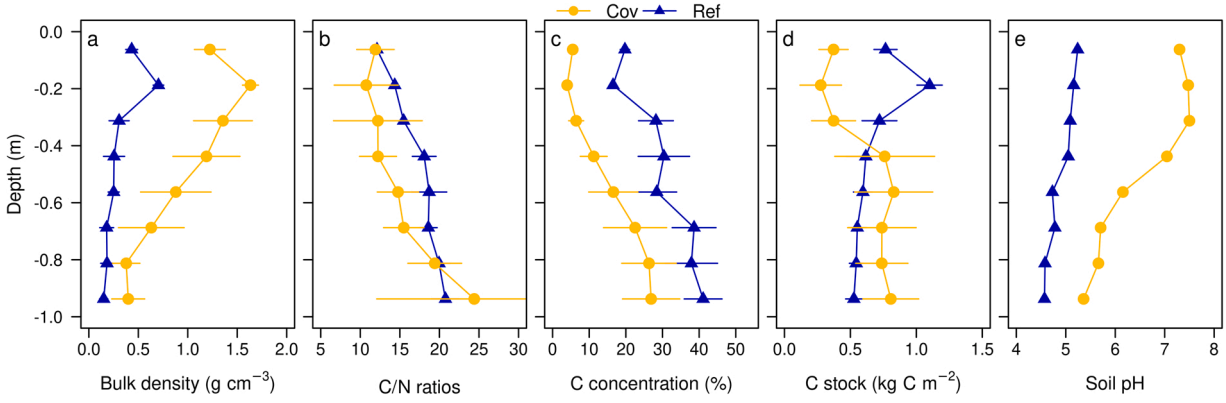

Fig. 2. Soil characteristics of the Rüthi site with (Cov) and without a mineral soil cover (Ref): a) soil bulk density, b) C/N ratios, c) SOC concentration, d) SOC stock (mean ± 2SE, n = 12) and e) pH (based on pooled samples).

5TE and GSM3 decagon devices, NE Hopkins Court, USA) at 0.05 m depth at Ref and Cov (Fig. 1). Missing soil moisture and temperature data—due to a failure in a single measurement device—were gap-filled (1 March 2018–7 May 2018, 4 November 2019–3 December 2019, 13 January 2010–23 January 2010 and 3 February 2020–5 May 2020) by performing a regression between the two sites. GWT depth was monitored by an observation well with a pressure transducer. Missing GWT data—due to a failure in a single measurement device (Cov: 13 January 2020–23 January 2020, Ref: 24 July 2018–31. August 2018, 08 October–11 October 2019, 14 October 2019–16 October 2019, 25 October 2019–03 December 2019 and 21 March 2020–16 June 2020)—were interpolated by performing a regression between two individual GWT measurements. Meanwhile, aerated SOC (SOC_{air}) stocks were calculated from GWT (annual and for the period May–September), bulk density and the SOC concentration by integrating over soil layers i with a layer depth z_i, as follows:

$$SOC_{air} = \sum_{i=1}^{i(GWT)} \rho_{d,i} \times SOC_i \times \Delta z_i \quad (3)$$

To compare the results herein with those in the literature, a depth profile of the bulk density and carbon concentration were extracted from the literature, and annual SOC_{air} stocks were calculated according to Eq. 3.

2.4. Determination of carbon exchange via harvest and fertilisers

The average mass of the harvested biomass was generally determined by weighing the total biomass from three subplots of 70 m^2 per field (Ref, Cov). A composite sample was taken from each subplot, packaged in an airtight container, weighed in the field and dried at 60°C in the laboratory to determine the Ref and Cov dry mass fraction, and the vegetation samples were measured for their total carbon and nitrogen content by elemental analysis (Hekatech, Germany).

2.5. CO_2 flux measurements and calculations

The net exchange of CO_2 between the ecosystem and atmosphere was measured using the EC method. A system was installed at Ref and Cov, consisting of a three-dimensional sonic anemometer (CSAT-3, Campbell Scientific UK) to measure directional wind velocities and temperature. Fast-response open-path infrared gas analysers were used to measure CO_2 (non-dispersive infrared spectroscopy, Li-7500a, Li7500 and Li7500RS, LI-COR Biosciences, Lincoln, USA). Further, the EC system was installed on a tripod tower 2.15 m above the ground, and data were recorded at a frequency of 10 Hz. Biannually, the zero and the span of the CO_2 analyser were set using high-purity N_2 zero gas and two standards with contrasting CO_2 concentrations (346 and 495 ppm for CO_2). Due to a breakdown of the EC system at Cov, no CO_2 measurements are available from 19 August 2018–28 October 2018. In 2019, a malfunction of the EC system at the Ref site led to a data gap from 24 April 2019–14 June 2019. Data gaps were filled according to the procedure described below.

A statistical test for raw data screening was conducted according to Vickers and Mahrt (1997), and half-hourly mean CO_2 fluxes were calculated from high-frequency data using the EC software EddyPro™ 7.0.9 (LI-COR Inc., Lincoln, Nebraska, USA), applying a 2-D wind vector rotation and linear detrending (Gash and Culf, 1996). Air density fluctuations were compensated for according to (Webb et al., 1980), and time lags were compensated for using the covariance maximisation method. To correct flux estimates for low- and high-frequency losses due to the instrument setup, intrinsic sampling limits of the method, according to Moncrieff et al. (1997) and Moncrieff et al. (2004), were used. In addition, calculated fluxes were quality flagged for micrometeorological tests, according to Mauder and Foken (2006), with flag values indicating 0 (best quality), 1 (suitable for annual budgets), and 2 (bad quality). CO_2 fluxes were removed when: (a) the quality flag was = 2, (b) the CO_2 signal strength was < 90 % (Li7500A) or > 70 % (Li7500), (c) the rotation angle for tilt correction was < 7 or > −7, (d) u*< 0.09, (e) the time lag for CO_2 < −0.7 s or > 0.7 s, (f) single valid values of QC or u* and (g) a variation in the CO_2 concentration > 0.5. In addition, based on the relationship between soil temperature and NEE measured at night, a temperature-dependent threshold for implausibly high positive (or negative) CO_2 fluxes was used to remove outliers.

2.6. CO_2 flux gap-filling and uncertainty estimation of annual sums

To obtain an annual budget, gaps in CO_2 fluxes were filled using the R program ReddyProc (Reichstein et al., 2005; Wutzler et al., 2018). The environmental factors used for gap filling were as follows: global radiation, soil temperature at 0.05 m depth and the vapour pressure deficit, and the tool provides a look-up table. Gap filling was performed based on similar meteorological conditions, and the time window against which the method looks for similar results is seven days. In the absence of similar conditions, the window is extended to 14 days, and the uncertainty of annual NEE estimates increases with the length of the data gap. Long periods without data (> one week), including cutting events, are especially problematic, as the gap-filling procedure does not reflect the reduced carbon assimilation after harvest (Wall et al., 2020). Therefore, for the two longest data gaps in 2018 and 2019, an alternative approach was used to fill the missing data. As a conservative approach that assumes no differences between the two sites, data from the other site were used (NEE from the reference site was used for the gap 1 August 2018–28 October 2018 of the cover fill site, and NEE from the cover fill site was used to close the gap from 24 April 2019–14 June 2019 of the reference site).

For the uncertainty evaluation of the NEE, we considered the two most essential error sources (Paul et al., 2021), and we determined that adding artificial gaps to the existing dataset estimates the uncertainty due to larger gaps. The five most significant gaps of other years were additionally inserted for each measurement year, whereas the systematic uncertainty of u* filtering was determined by varying the u* threshold prior to gap-filling within a range of – 0.04 and + 0.04 m s^{-1} around the chosen threshold. The 95 % confidence interval (CI) of the NEE according to the u* threshold was estimated using the average deviation for the lowest and highest u* thresholds for all years, whereas the 95 % CI of the NEE due to gaps was estimated using the average deviation caused by inserting artificial gaps. The uncertainty surrounding annual carbon exports was calculated by combining the individual uncertainties of each cutting event using Gaussian error propagation. The uncertainty of carbon input for individual years was estimated using the average standard deviation of all fertilisation events and combining individual uncertainties using Gaussian error propagation. Thus, the total uncertainty of the NECB was subsequently calculated by combining the individual uncertainties using Gaussian error propagation.

2.7. N_2O and CH_4 flux measurements and data processing

N_2O and CH_4 fluxes were measured continuously with eight custom-built automatic chambers and associated controller systems, according to Wang et al. (2022). In brief, steel chambers (0.3×0.3×0.22 m) were automatically closed every few hours (2–9 hours) for 15 min. Headspace gas samples were collected at four time points during chamber closure and stored in four corresponding gasbags (Supel™, USA). The collected samples (integrating N_2O emissions over periods between 0.5 and 2 weeks) were regularly measured in the lab with a Picarro QCL (G2308, Picarro, USA). In addition, a CO_2 sensor (Senseair, Sweden) installed within the chamber measured the real-time CO_2 concentration increase in the chamber's headspace to check the tightness of the closure.

N_2O and CH_4 chamber fluxes were calculated according to Wang et al. (2022), where gas fluxes during each chamber closure were

evaluated by linear regression. Further, N_2O and CH_4 fluxes calculated from the concentration gradient of the gasbags were selected for post-processing after fulfilling specific quality criteria. First, the R^2 of the CO_2 fluxes calculated from the regression lines of the four bags had to exceed 0.9, indicating that within the sampling days, the ATIC worked adequately. In addition, $R^2 \leq 0.9$ indicated a failure in gas sampling on the sampling days, which led to the rejection of the flux data. Second, an $R^2 > 0.9$ of the N_2O and an R^2 of >0.8 of the CH_4 regression lines were considered critical to accept the data for further analysis. However, low fluxes (within $\pm$ 0.5 mg N m^{-2} day^{-1}; $\pm$ 0.2 mg C m^{-2} day^{-1}, for N_2O and CH_4, respectively; calculated based on the detection limit of the Picarro) were accepted regardless of the R^2. Overall, N_2O data covered 91 % for Ref and 90 % for Ref and Cov, whereas CH_4 data covered 61 % and 54 % of the experimental period for Ref and Cov, respectively.

The gaps in the N_2O and CH_4 fluxes were also filled, according to Wang et al. (2022). To determine annual N_2O and CH_4 exchange values, the time series for each chamber was individually gap-filled before being combined with site averages. Missing flux values due to a failure of the chamber system or data rejection were filled by two different strategies according to management events. Fertilisation-induced emissions were defined as the time period with higher emissions after the fertilisation event, which was higher than two weeks before fertilisation for N_2O, and higher than the sampling campaign when slurry was applied for CH_4 emission. Concerning the failure of individual chambers during these fertilisation events, mean values from the properly operating chambers at each site were used to fill the data gaps. For missing values outside fertilisation events, a look-up table approach with two parameters (soil moisture and soil temperature) was used to fit the missing values (RMSE = 0.54 mg N m^{-2} day^{-1}, $R^2 = 0.44$ and RMSE = 0.009 mg C m^{-2} day^{-1}, $R^2 = 0.57$), for N_2O and CH_4, respectively. Finally, the annual cumulative fluxes of each chamber were averaged for the two sites, Ref and Cov, whereas the uncertainty was estimated from the variation in the four repetition chambers per site.

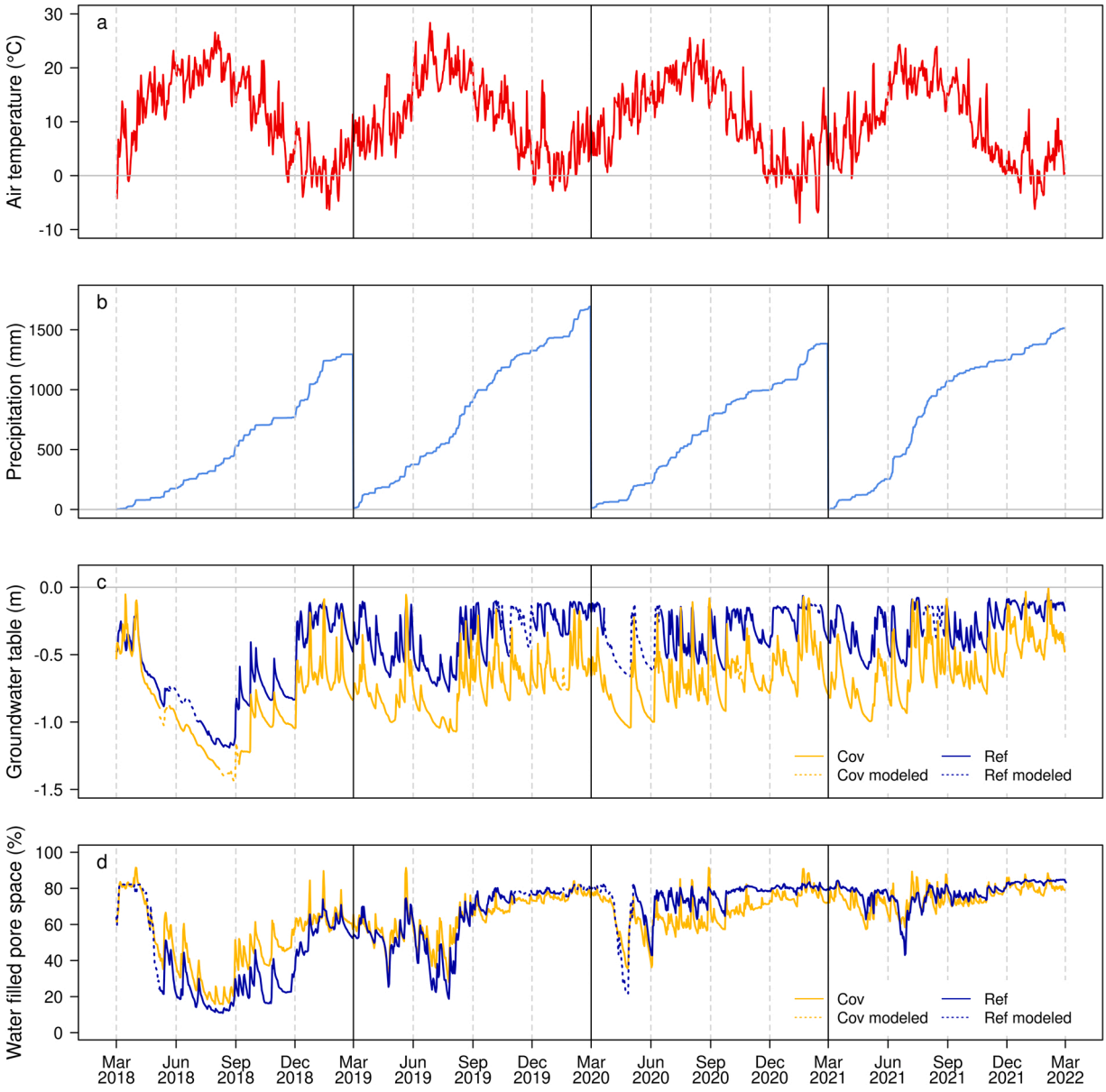

Fig. 3. Environmental conditions for without (Ref) and with (Cov) mineral soil coverage: a) air temperature, b) annual cumulative precipitation, c) daily groundwater table (GWT) depth and d) water-filled pore space at 0.05 m depth.

3. Results

3.1. Environmental conditions and management

The mean annual air temperature during the four-year measurement campaign varied between 9.5°C (Year 4) and 11.2°C (Year 1, Fig. 3a). Cumulative annual precipitation varied between 1300 mm in Year 1 and 1687 mm in Year 2 (Fig. 3b). The summer of Year 1 was the driest, whereas the summer of Year 4 was the wettest of the four years. Accordingly, the lowest mean annual GWT was measured in Year 1 with −0.65 m at Ref and −0.89 m at Cov (Fig. 3c), and the following three years were characterised by higher mean annual GWT levels of −0.36 m, −0.33 m and −0.28 m at Ref and −0.72 m, −0.67 m and −0.56 m at Cov. All four years were characterised by annual variations in humidity, with drier conditions during summer and wetter conditions in wintertime. Yet, the dry Year 1 showed the lowest waterfilled pore space in the summer (28 % for Cov and 18 % for Ref), while in Year 4, a relatively high proportion of pore space (up to 72 %) was also filled in the summer (Fig. 3d).

At both sites, the grassland was fertilised identically with slurry and mineral fertiliser three to five times per year, resulting in a four-year average input of 146 ± 9 g C m^{-2} $year^{-1}$ and 26 ± 1 g N m^{-2} $year^{-1}$ (Fig. 4a, Table S1). The grass was harvested five to six times annually, with the yield varying from 363 ± 28 to 449 ± 33 g C m^{-2} $year^{-1}$ for Ref and from 404 ± 40 to 529 ± 23 g C m^{-2} $year^{-1}$ for Cov (Fig. 4a, Table 1). Further, the four-year average yield of Cov (460 ± 17 g C m^{-2} $year^{-1}$) was slightly higher than for Ref (412 ± 14 g C m^{-2} $year^{-1}$ Table 1). The yield was unrelated to the GWT.

3.2. Gas fluxes

At both sites, the cumulative NEE showed high inter-annual variability, ranging from 537 ± 68 g C m^{-2} $year^{-1}$ in the first dry year to −92 ± 92 g C m^{-2} $year^{-1}$ in the fourth year. Compared to the high variations among the different years, the influence of soil coverage on NEE was small and insignificant (Fig. 4b; Table 1). Daily NEE was generally negative in the springtime, dominated by the carbon uptake of the growing vegetation, and it turned positive in the summertime, although the extent of the increase varied considerably over the period assessed.

Annual CH_4 exchange rates were consistently low at both sites, with CH_4 uptake dominating. The average CH_4 uptake was slightly higher at Cov than at Ref (-0.04 ± 0.02 g CH_4-C m^{-2} $year^{-1}$ and −0.07 ± 0.01 g CH_4-C m^{-2} $year^{-1}$), but the values did not differ across the period assessed (Table 1).

In Year 4, total N_2O emissions amounted to 0.41 ± 0.09 g N m^{-2} $year^{-1}$ for Ref and 0.12 ± 0.02 g N m^{-2} $year^{-1}$ for Cov (Figure S2), and considerably higher cumulative annual N_2O emissions were measured in Years 2 and 3 at both sites (3.27 ± 0.78 g N m^{-2} $year^{-1}$ [mean and 2SE] and 0.83 ± 0.34 g N m^{-2} $year^{-1}$ [Ref] and 0.32 ± 0.08 and 0.13 ± 0.04 g N m^{-2} $year^{-1}$ [Cov]; Wang et al., 2022). The three-year average of total N_2O emissions was 1.50 ± 0.73 g N m^{-2} $year^{-1}$ for Ref and 0.10 ± 0.05 g N m^{-2} $year^{-1}$ for Cov.

3.3. Carbon budget

The NECB varied considerably among the different years, regardless of the soil coverage: NECB was highest in Year 1 (786 ± 75 g C m^{-2} $year^{-1}$ [Ref] and 826 ± 100 g C m^{-2} $year^{-1}$ [Cov]) and lowest in Year 4 (175 ± 75 g C m^{-2} $year^{-1}$ [Ref] and 125 ± 102 g C m^{-2} $year^{-1}$ [Cov]; Table 1). The high interannual variability was mainly caused by the high variability in NEE at both sites, as the other components of the NECB were—compared to the NEE—relatively constant at both sites.

The variability in the NECB was related to the GWT, where the lower the GWT depth, the higher the loss at Cov and Ref (Fig. 5a). However, a lower GWT of, on average, 0.3 m at Cov did not induce additional SOC mineralisation. Indeed, the soil coverage did not significantly change the SOC losses at the drained peatland: the four-year averaged NECB was the same for Ref (463 ± 38 g C m^{-2} $year^{-1}$) and Cov (454 ± 50 g C m^{-2} $year^{-1}$) and differences between Ref and Cov were small and insignificant. When plotted against aerated SOC_{air} in the summer, the NECB showed the same response at both sites, independent of the coverage (Fig. 5b).

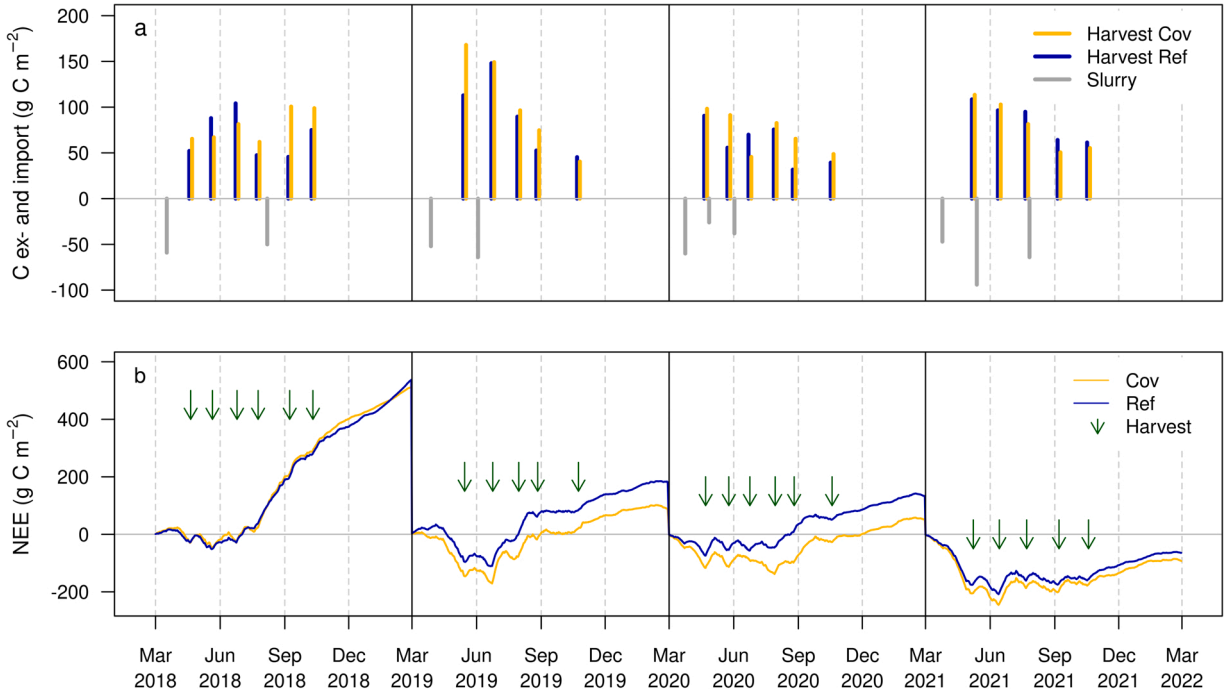

Fig. 4. Carbon components of the net ecosystem carbon budget (NECB) without (Ref) and with (Cov) mineral soil coverage: (a) harvest and slurry and (b) cumulative net ecosystem exchange (NEE) over the four years assessed. Negative numbers mean carbon import (uptake) and positive numbers mean export (emission).

Table 1
Carbon budget components and net ecosystem carbon budget (NECB) (g C m^{-2} $year^{-1}$), and their 95 % confidence intervals (CIs; ~2 SE) at the site without (Ref) and with soil coverage (Cov) for the four measurement years. Different lower-case letters represent a significant difference between Ref and Cov within the same year, and different upper-case letters represent a significant difference between the components of Ref or Cov across the four years.

		Year 1	Year 2	Year 3	Year 4	**Mean**
NEE	Ref	537 (68)^{aA}	181 (68)^{aB}	132 (68)^{aB}	−64 (68)^{aC}	**197 (34)^{a}**
NEE	Cov	512 (92)^{aA}	87 (92)^{aB}	52 (92)^{aAB}	−92 (92)^{aC}	**140 (46)^{b}**
CH_4	Ref		−0.05 (0.02) ^{aA}	−0.01 (0.03)^{aA}	−0.05 (0.03)^{aAB}	**−0.04 (0.02)$^{a\ x}$**
CH_4	Cov		−0.04 (0.02)^{aA}	−0.07 (0.02)^{bAB}	−0.09 (0.02)^{aB}	**−0.07 (0.01)$^{b\ x}$**
C_{input}	Ref	−161 (19)^{aA}	−124 (15)^{aB}	−111 (19)^{aB}	−187 (19)^{aA}	**−146 (9)^{a}**
C_{input}	Cov	−161 (19)^{aA}	−124 (15)^{aB}	−111 (19)^{aB}	−187 (19)^{aA}	**−146 (9)^{a}**
C_{export}	Ref	410 (24)^{aA}	449 (33)^{aA}	363 (28)^{aB}	426 (24)^{aAC}	**412 (14)^{a}**
C_{export}	Cov	475 (35)^{bA}	529 (23)^{bA}	432 (39)^{bB}	404 (40)^{aC}	**460 (17)^{b}**
NECB	Ref	786 (75)^{aA}	506 (77)^{aB}	384 (76)^{aC}	175 (75)^{aD}	**463 (38)^{a}**
NECB	Cov	826 (100)^{aA}	492 (96)^{aB}	373 (102)^{aBC}	125 (102)^{aD}	**454 (50)^{a}**

^{x}To calculate the four-year average and the NECB of Year 1, the missing data (CH_4 Year 1) were replaced by the average value of the subsequent three years.

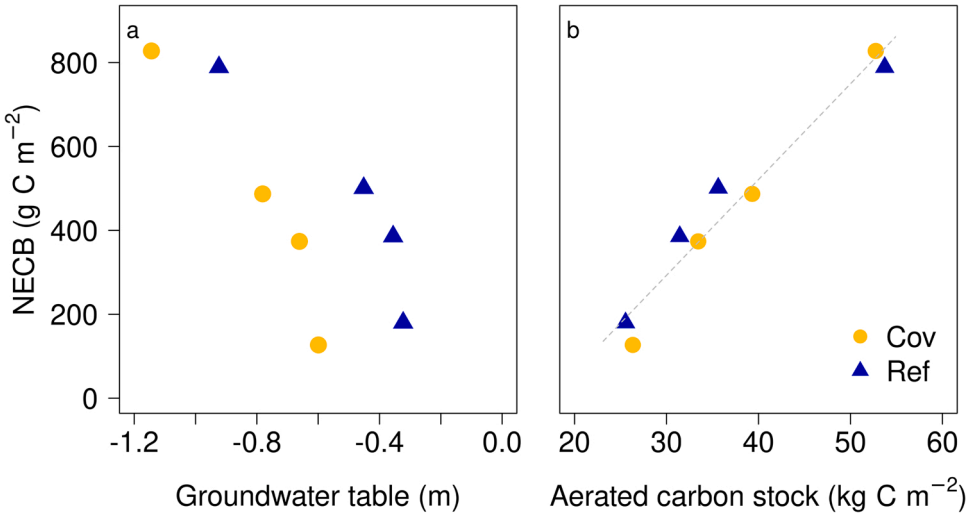

Fig. 5. Response of Net Ecosystem Carbon Budget (NECB) to (a) mean groundwater table depth from May to September and to b) the aerated soil organic carbon stock (SOC_{air}) from May to September (NECB = 22.8*SOC_{air} - 392; R^2 = 0.96) for the site without (Ref) and with (Cov) mineral soil coverage.

3.3.1. *GHG budget*

Because a full GHG budget is only available for Years 2–4, the evaluation of the different components of the full GHG budget was done using these three years. The average GHG emission of Ref was 19.2 ± 2.0 t CO_2 eq. ha^{-1} $year^{-1}$, and it was dominated by the NECB (73 %) and, to a smaller extent, by N_2O emissions (27 %), whereas CH_4 emissions contributed marginally (<0.1 %) to total GHG emissions (Fig. 6). Covering the peatland with a mineral soil layer reduced GHG emissions by 6.4 t CO_2 eq. ha^{-1} $year^{-1}$ which was mainly related to the effect of soil coverage on N_2O emissions. However, not only did absolute N_2O emissions vary considerably between Year 2 and Years 3 and 4, but also their relative contribution to total GHG emissions: For Year 2, N_2O emissions contributed about 43 % of the full GHG budget at Ref. In the two following years, the contribution of N_2O to the total emission was considerably lower (20 % and 21 %). Thus, the effect of soil coverage on N_2O emissions was less pronounced in Years 3 and 4, as were the contributions of N_2O to total GHG emissions. At Cov, NECB contributed, on average, more than 93 % to the GHG budget, while N_2O and CH_4 emissions contributed only 6 % and <0.3 %, respectively. Further, compared to NECB and N_2O emissions, CH_4 emissions did not influence overall GHG emissions.

4. Discussion

4.1. *SOC losses without mineral soil layer*

SOC losses from the non-covered organic soil (Ref, 463 ± 38 g C m^{-2} $year^{-1}$) with an average GWT of −0.41 m are at the lower end of the deeply drained peatlands of the temperate zone (Hiraishi et al., 2014; Tiemeyer et al., 2020; Evans et al., 2021). This four-year average lies within the same range as the long-term integrated SOC loss rates since the onset of peat drainage of the sites in 1890 CE (310– 630 g C m^{-2} $year^{-1}$), as revealed by the ^{14}C approach (Wang et al., 2021).

We observed a clear increase in annual SOC losses with a deeper GWT, in line with the literature (Leiber-Sauheitl et al., 2014; Fortuniak et al., 2017; Hirano et al., 2012). However, the response of the GWT to SOC losses is highly variable across meta-studies, and a linear (Couwenberg and Fritz, 2012; Evans et al., 2021) or sigmoidal relationship was proposed (Tiemeyer et al., 2020; Koch et al., 2023). Tiemeyer et al. (2020) attributed the high variation partly to differences in nutrient status and intra-annual GWT dynamics between and within sites. Boonman et al. (2022) showed that the summer GWT better predicts SOC losses than the annual GWT from Dutch grasslands. As peat mineralisation is temperature-dependent, the GWT in summer is more crucial than in the cold season, when mineralisation rates are low. At our site, the summer and the annual GWT (data not shown) can predict the annual soil carbon losses at both sites; however, a different response function must be used for Ref and Cov. In addition to these factors, differences in peat quality may add to the observed variation (Paul and Leifeld, 2023). Land use intensity might also contribute to the observed variations in the relatively low SOC losses among grasslands in the UK (Evans et al., 2021). Moreover, land use history may also contribute to the observed variations among different sites.

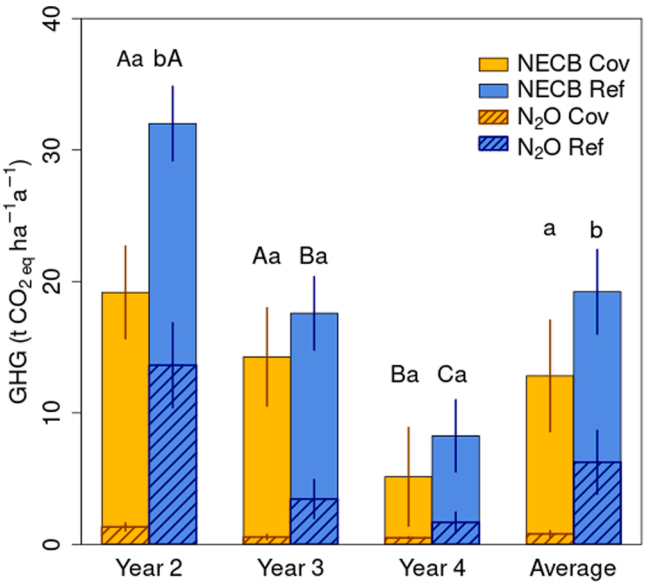

Fig. 6. GHG fluxes and their 95 % CIs for the site without (Ref) and with (Cov) mineral soil coverage, but CH_4 emissions are too small for visualisation. Different lower-case letters represent a significant difference between Ref and Cov within the same year, whereas different upper-case letters represent a significant difference between the components of Ref or Cov across the three years.

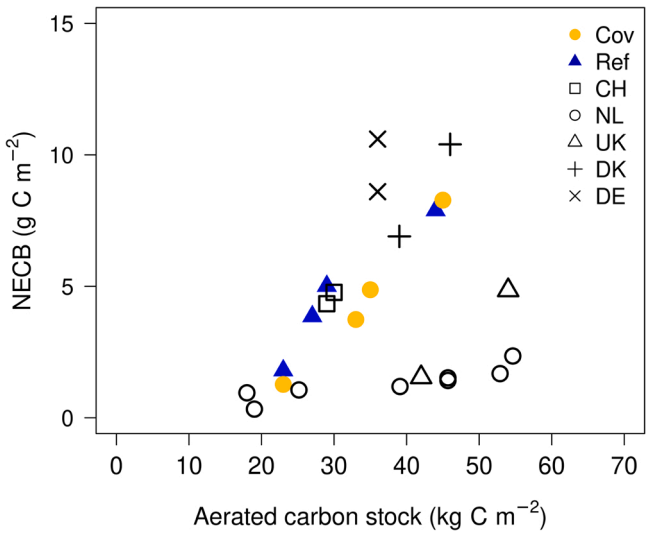

Fig. 7. Response of net ecosystem exchange budget (NECB) to annual aerated carbon stock (SOC_{air}) of organic soils under grassland (Cov and Ref of this study; with NECB = 27.8*SOC_{air} - 449; R^2= 0.90) and literature data (CH: Paul et al., 2021; NL: Boonman et al., 2022 and Hefting et al., 2022, UK: Evans et al., 2021, Evans et al., 2016b; DE: Leiber-Sauheitl et al., 2014 and Poyda et al., 2016; DK: Elsgaard et al., 2012 and Schäfer et al., 2012).

4.2. *Influence of soil coverage and aerated SOC stock on SOC losses*

Covering the drained organic soil with a mineral layer did not reduce the SOC losses in any of the four years assessed, with an average SOC loss (454 ± 50 g C m^{-2} $year^{-1}$) at a GWT of −0.72 m, which is lower than emissions from peatlands in the UK (792 g C m^{-2} $year^{-1}$; Evans et al., 2021) and Germany (1006 g C m^{-2} $year^{-1}$; Tiemeyer et al., 2020). To identify reasonable predictors of CO_2 emissions from drained peatland, SOC losses may be related not only to the GWT but also to the amount of aerated SOC, which is, in addition to the GWT, also defined by the SOC concentration and soil bulk density. Following the approach of summer GWT, we calculated the summer SOC_{air} stock, which precisely determines the SOC loss rate independently of the soil coverage (Fig. 5b). Compared to the annual SOC_{air} stock, summer SOC_{air} stock showed a higher coefficient of determination (Figs. 5 and 7), where about 1.4–1.3 % of the aerated SOC stock is released at Ref and Cov in Years 1–3, while in Year 4, slightly lower amounts of 0.7 % and 0.5 % at Ref and Cov are lost. In Year 4, only the topsoil was aerated, and consequently, highly degraded peat material, is suspected to be more stable, was mineralised. Together, we argue that at our site, the SOC_{air} stock is a better indicator of SOC losses than GWT. To test whether SOC_{air} is a more suitable indicator of SOC loss than GWT in general, we extend the data base by adding further data from the literature (Fig. 7). While a similar function could be used for other degraded organic soils under grasslands in Switzerland, an overall valid relationship seems non-existent (Fig. 7). We therefore suggest using SOC_{air} stocks rather than GWT if predictions of C-losses for individual sites are envisaged.

In addition to changing the amount of SOC_{air}, the mineral soil coverage also influences other important drivers of microbial activity. In particular, soil temperature and pH differences could modify the carbon mineralisation rates at Cov and Ref. Regarding temperature, we found no difference in the summer soil temperature, though the alkaline mineral cover increased the pH of the top peat from around 5.2–6.1 beneath the soil cover. Incubation experiments revealed that adding lime to the peat samples increased the pH and carbon mineralisation rates (Ivarson, 1977; Bergman et al., 1999). Thus, a higher pH of the peat at Cov may increase peat mineralisation rates. However, this effect may be counteracted by the slight compaction of the peat under the mineral soil layer or be of minor importance, as the loss rates for Ref and Cov were the same.

In mineral soils, soil organic matter is stabilised through interactions with the mineral soil phase (von Lützow et al., 2008), and clay content is one major factor controlling the carbon content in mineral soils (Paul et al., 2008; Poeplau et al., 2020). Thus, theoretically, adding mineral soil with a relatively low carbon content could offer binding sites for SOC stabilisation. After 12 years of intensive grassland management, SOC contents were indeed higher in the upper part of the mineral soil cover (3.5 ± 1.0 % vs 1.5 ± 0.6 % [mean and 2SE, Fig. 2]), indicating recent SOC accumulation. Thus, to estimate the carbon sequestration potential of the mineral soil cover at Rüthi, the average carbon concentration of Swiss grasslands with identical clay content was calculated according to Leifeld et al. (2005). A carbon concentration of 2.2 % (0–0.3 m) of the soil cover falls into the same range as the average of Swiss grasslands (2.0±0.6 %), and SOC stocks (0–0.3 m) are similar (87 ±28 t C ha^{-1} Cov; 86±27 t C ha^{-1} average of Swiss mineral grasslands). We, therefore, consider it unlikely that a relevant amount of SOC will be additionally sequestered in the mineral soil cover. In summary, the aerated summer carbon stock is the overriding factor determining SOC loss at both sites.

4.3. *Soil coverage as a mitigating measure*

Overall, we found no effect of mineral soil coverage on the NECB at our sites, the literature also supports this missing effect of a mineral soil cover on SOC loss from drained peatlands. Incubation experiments showed that peat and peat–sand mixtures had comparable specific CO_2 fluxes (i.e., fluxes normalised by the sample's SOC stock; Säurich et al., 2019). In addition, field experiments in the Netherlands showed that SOC loss from peat soils with a naturally occurring clay layer did not differ systematically from those without clay (Weideveld et al., 2021; Veenendaal et al., 2007). Furthermore, organic soils mixed with sand, resulting in a SOC content of about 10 %, emitted carbon within a similar range as peat soils without soil amendments and a high SOC content (Tiemeyer et al., 2016).

Overall, the NECB dominated the GHG budget of our drained, intensively used grasslands with and without soil cover, followed by

N_2O. Compared to these fluxes, the contribution of CH_4 uptake to total GHG emissions is negligible. As SOC loss was unaffected by the mineral soil cover, the mitigation effect was limited to N_2O; thus, soil coverage considerably reduced N_2O emissions in all three measurement years. The N_2O reduction could be assigned to differences in topsoil properties, namely the combination of a higher pH, a lower SOC content and available N in the topsoil of Cov (Wang et al., 2022). A similar effect was reported by Wüst-Galley et al. (2023), who observed reduced N_2O emissions from a mineral soil cover for temperate rice cropping on organic soil.

N_2O emissions at Cov lie within the range of N_2O emissions for fertilised grasslands on mineral soils in Switzerland (Ammann et al., 2020; Merbold et al., 2021; Fuchs et al., 2020), while N_2O emissions at Ref were in line with rates from intensively used organic soils with a high N-fertiliser input in Germany (Tiemeyer et al., 2020), and they correspond with previous estimates for drained organic soils in Switzerland (Leifeld, 2018). This supports the assumption that N_2O produced in the peat underneath the mineral soil cover does not contribute significantly to N_2O emissions at Cov. Indeed, Neftel et al. (2000) showed that N_2O emissions originate mainly from the topsoil. Accordingly, N_2O emissions at Cov are independent of the underlying peat. In line with this, about 0.8 % of the applied N fertiliser is emitted as N_2O from Cov, which is close to the IPCC emissions factor of 1 % (2014). In organic soils, additional N is available from peat mineralisation, accounting for 200 kg N ha^{-1} (300, 200 and 100 kg for Years 2, 3 and 4) at our site. At Ref, the amount of N emitted as N_2O corresponds to about 3 % of the N input from fertiliser and N mineralisation or 7 % of the N input from fertiliser alone. We are missing an unfertilised control plot, so we cannot calculate the N_2O emissions produced exclusively by fertilisation. Measurements from Dutch peatlands, including an unfertilised control, revealed an emission factor of 3 % (Velthof and Rietra, 2018), suggesting that fertiliser-induced N_2O emissions are higher in organic soils than in mineral soils.

N_2O fluxes are characterised by high inter-annual variability, as for extremely high N_2O emissions, multiple factors must interact simultaneously (Dobbie et al., 1999). High soil temperature, fertiliser application and a specific soil humidity, along with the preceding dry period, were responsible for high peak emissions in Year 2 (Wang et al., 2022), whereas N_2O emissions from that year represented almost half the total GHG release at Ref. In the following two years, N_2O emissions contributed still about 20 % to total GHG emissions, and a similar contribution was reported from grasslands with N-fertiliser inputs > 15 g N m^2 $year^{-1}$ in German peatlands (Tiemeyer et al., 2020). For comparison, in the Netherlands, clayey peat soils or peatlands with a clay surface layer of 0.25 m thickness emitted 1.5 g N m^{-2} $year^{-1}$, indicating that not all mineral layers are equally suited to lower N_2O emissions (Kroon et al., 2010). Given the high mitigation potential revealed in this study, more research is needed on the optimal properties of the mineral soil layer, including thickness, texture, SOC content, pH and humidity or GWT, to reduce N_2O emissions efficiently from drained organic soils.

5. Conclusion

Covering drained organic soil with a mineral soil layer did not decrease SOC loss, as the latter is driven by the size of the aerated carbon stock. This implies that a reduction in SOC losses may only be achieved by raising the GWT (relative to the peat surface), which is clearly facilitated by a mineral cover layer, as the latter increases the carrying capacity of the soil and provides a non-saturated topsoil. This allows regular agricultural production, i.e. cultivation of crops not adapted to wet conditions, and grassland yields could even slightly improve due to soil coverage. Moreover, by choosing a suitable mineral layer, N_2O emissions can also be reduced.

In practice, the feasibility of this mitigation option is limited mainly by two factors: the availability of mineral soil material and the management of an optimal GWT. While mineral soil material is a non-renewable resource, thus valuable and limited, many construction sites produce residual soil. In Switzerland, governmental ordinance requires that uncontaminated excavated top- and subsoil be reused for soil improvement measures such as recultivation or melioration of agricultural soils. If such material is available within a reasonable distance to drained organic soils, it is often used as mineral soil cover without considerable impact on the sustainability of the mitigation measure. Otherwise, the additional emissions and other potential environmental impacts due to the translocation of the soil material would need to be taken into account (e.g., by a life cycle assessment). Mechanical peat properties might prevent adding thick mineral layers to all organic soils, as the soil's carrying capacity is limited and the soil is prone to compaction (Ochselin et al., 2023). Adjusting to a specific GWT level over the years requires technical knowledge and specific installations. Implementing it in all peatlands and every year may be challenging, as a relatively dense network of sub-irrigation pipes is required to maintain a stable GWT in the field (Kechavarzi et al., 2007). In addition, sufficient water reservoirs are needed for dry periods. Therefore, achieving optimal GWT levels every year may not be possible. Hence, covering the organic soil might extend the period for intensive grassland management without renewing the drainage system. However, SOC loss and subsidence will continue even if only part of the peat layer is not water-saturated. The use of mineral soil coverage on intensively used drained peatlands, which are unsuitable for rewetting due to soil conditions or socioeconomic constraints, may therefore be a management strategy to prolong the agricultural usability of organic soils by dry cultivation, reduce SOC loss as long as the water table is considerably raised, and thus postpone corresponding CO_2 emissions until the future, as a time-saving option.

CRediT authorship contribution statement

Christof Ammann: Writing – review & editing, Methodology. **Sonja Paul:** Writing – original draft, Project administration, Investigation, Funding acquisition, Conceptualization. **Christine Alewell:** Writing – review & editing, Conceptualization. **Yuqiao Wang:** Writing – review & editing, Visualization, Methodology. **Jens Leifeld:** Writing – review & editing, Funding acquisition, Conceptualization.

Declaration of Competing Interest

The authors declare that they have no known competing financial interests or personal relationships that could have appeared to influence the work reported in this paper.

Data Availability

Data will be made available on request.

Acknowledgements

We gratefully acknowledge the financial support of the Federal Office for the Environment (BAFU 16.0152.PJ / Q062-0784 and 16.0152.PJ / BAFU-D-BF3A3401/781), especially we would like to thank Andreas Schellenberger for the continuous support and engagement for the project. We are also expressing our gratitude to Markus Jocher and Steven Nagel for their technical support and fieldwork. Finally, we are very grateful to the farmer, Bernhard Schneider, for the excellent cooperation.

Appendix A. Supporting information

Supplementary data associated with this article can be found in the online version at doi:10.1016/j.agee.2024.109197.

References

Ammann, C., Neftel, A., Jocher, M., Fuhrer, J., Leifeld, J., 2020. Effect of management and weather variations on the greenhouse gas budget of two grasslands during a 10-year experiment. Agric. Ecosyst. Environ. *292*, 106814.

Bambalov, N., 1999. Dynamic of organic matter in peat soil and under the conditions of sand-mix culture during 15 years. Int. Agrophys. *13*, 269–272.

Bergman, I., Lundberg, P., Nilsson, M., 1999. Microbial carbon mineralisation in an acid surface peat: effects of environmental factors in laboratory incubations. Soil Biol. Biochem. *31* (13), 1867–1877.

Beyer, C. (2014). Greenhouse gas exchange of organic soils in northwest Germany: effects of organic soil cultivation, agricultural land use and restoration [PhD thesis, Universität Bremen]. <⟨http://nbn-resolving.de /urn:nbn:de:gbv:46-00103939-13⟩> Accessed 04/10/2024.

Blankenburg, J., 2015. Die landwirtschaftliche Nutzung von Mooren in Nordwestdeutschland. Telma *5*, 29–58.

Boonman, J., Hefting, M.M., van Huissteden, C.J.A., van den Berg, M., van Huissteden, J., Erkens, G., Melman, R., van der Velde, Y., 2022. Cutting peatland CO2 emissions with water management practices. Biogeosciences *19*, 5707–5727.

Carlson, K.M., Gerber, J.S., Mueller, N.D., Herrero, M., MacDonald, G.K., Brauman, K.A., Havlik, P., O'Connell, C.S., Johnson, J.A., Saatchi, S., West, P.C., 2017. Greenhouse gas emissions intensity of global croplands. Nat. Clim. Chang *7* (1), 63–68.

Chapin, F.S., Woodwell, G.M., Randerson, J.T., Rastetter, E.B., Lovett, G.M., Baldocchi, D.D., Clark, D.A., Harmon, M.E., Schimel, D.S., Valentini, R., Wirth, C., Aber, J.D., Cole, J.J., Goulden, M.L., Harden, J.W., Heimann, M., Howarth, R.W., Matson, P.A., McGuire, A.D., Melillo, J.M., Mooney, H.A., Neff, J.C., Houghton, R.A., Pace, M.L., Ryan, M.G., Running, S.W., Sala, O.E., Schlesinger, W.H., Schulze, E.-D., 2006. Reconciling carbon-cycle concepts, terminology, and methods. Ecosystems 9, 1041–1050.

Couwenberg, J., Fritz, C., 2012. Towards developing IPCC methane 'emission factors' for peatlands (organic soils). Mires Peat *10* (03), 1–17.

Darusman, T., Murdiyarso, D., Anas, I., 2023. Effect of rewetting degraded peatlands on carbon fluxes: A meta-analysis. Mitig. Adapt Strateg Glob. Chang *28* (3), 10.

Dobbie, K.E., McTaggart, I.P., Smith, K.A., 1999. Nitrous oxide emissions from intensive agricultural systems: variations between crops and seasons, key driving variables, and mean emission factors. J. Geophys Res Atmos. *104* (D21), 26891–26899.

Elsgaard, L., Görres, C.M., Hoffmann, C.C., Blicher-Mathiesen, G., Schelde, K., Petersen, S.O., 2012. Net ecosystem exchange of CO2 and carbon balance for eight temperate organic soils under agricultural management. Agric., Ecosyst. Environ. 162, 52–67.

Erkens, G., Van der Meulen, M.J., Middelkoop, H., 2016. Double trouble: Subsidence and CO2 respiration due to 1,000 years of Dutch coastal peatlands cultivation. Hydrogeol. J. *24* (3), 551.

Evans, C., Morrison, R., Burden, A., Williamson, J., Baird, A., Brown, E., Callaghan, N., Chapman, P., Cumming, A., Dean, H., Dixon, S., Dooling, G., Evans, J., Gauci, V., Grayson, R., Haddaway, N., He, Y., Heppell, K., Holden, J., Worrall, F., 2016b. Final report on project SP1210: Lowland peatland systems in England and Wales – evaluating greenhouse gas fluxes and carbon balances. Cent. Ecol. Hydrol. ⟨https://randd.defra.gov.uk/ProjectDetails?ProjectId=17584⟩ Accessed 04/10/2024.

Evans, C.D., Peacock, M., Baird, A.J., Artz, R.R.E., Burden, A., Callaghan, N., Chapman, P.J., Cooper, H.M., Coyle, M., Craig, E., Cumming, A., Dixon, S., Gauci, V., Grayson, R.P., Helfter, C., Heppell, C.M., Holden, J., Jones, D.L., Kaduk, J., Morrison, R., 2021. Overriding water table control on managed peatland greenhouse gas emissions. *Nature 593* (7860), 548–552.

Evans, C.D., Renou-Wilson, F., Strack, M., 2016a. The role of waterborne carbon in the greenhouse gas balance of drained and re-wetted peatlands. Aquat. Sci. *78*, 573–590.

Evans, C.D., Williamson, J.M., Kacaribu, F., Irawan, D., Suardiwerianto, Y., Hidayat, M. F., Laurén, A., Page, S.E., 2019. Rates and spatial variability of peat subsidence in Acacia plantation and forest landscapes in Sumatra, Indonesia. Geoderma *338*, 410–421.

Ferré, M., Muller, A., Leifeld, J., Bader, C., Müller, M., Engel, S., Wichmann, S., 2019. Sustainable management of cultivated peatlands in Switzerland: Insights, challenges, and opportunities. Land Use Policy *87*.

Fortuniak, K., Pawlak, W., Bednorz, L., Grygoruk, M., Siedlecki, M., Zieliński, M., 2017. Methane and carbon dioxide fluxes of a temperate mire in Central Europe. Agric. Meteor. *232*, 306–318.

Frank, S., Tiemeyer, B., Bechtold, M., Lücke, A., Bol, R., 2017. Effect of past peat cultivation practices on present dynamics of dissolved organic carbon. Sci. Total Environ. *574*, 1243–1253.

Fuchs, K., Merbold, L., Buchmann, N., Bretscher, D., Brilli, L., Fitton, N., Topp, C.F.E., Klumpp, K., Lieffering, M., Martin, R., Newton, P.C.D., Rees, R.M., Rolinski, S., Smith, P., Snow, V., 2020. Multimodel evaluation of nitrous oxide emissions from an intensively managed grassland. J. Geophys. Res.: Biogeosci. *125*. , e2019JG005261.

Gash, J.H.C., Culf, A.D., 1996. Applying a linear detrend to eddy correlation data in realtime. Bound. Layer Meteorol. 79 (3), 301–306.

Hefting, M.M., van Asselen, S., Keuskamp, J.A. Harpenslager, S.F. & Erkens, G. (2022). Carbon stocks in sight: High-resolution vertical depth profiles to quantify carbon reservoirs in the NOBV research sites. In *Chapter 12 NOBV Report 2022*. <⟨https://www.nobveenweiden.nl/en/⟩> Accessed 04/10/2024.

Hiraishi, T., Krug, T., Tanabe, K., Srivastava, N., Baasansuren, J., Fukuda, M., Troxler, T. G., 2014. 2013 Supplement to the 2006 IPCC Guidelines for National Greenhouse Gas Inventories: Wetlands (Eds.). Intergovernmental Panel on Climate Change, Switzerland.

Hirano, T., Segah, H., Kusin, K., Limin, S., Takahashi, H., Osaki, M., 2012. Effects of disturbances on the carbon balance of tropical peat swamp forests. Glob. Chang Biol. *18*, 3410–3422.

Ivarson, K.C., 1977. Changes in decomposition rate, microbial population and carbohydrate content of an acid peat bog after liming and reclamation. Can. J. Soil Sci. *57* (2), 129–137.

Kechavarzi, C., Dawson, Q., Leeds-Harrison, P.B., Szatyłowicz, J., Gnatowski, T., 2007. Water-table management in lowland UK peat soils and its potential impact on CO2 emission. Soil Use Manag *23* (4), 359–367.

Keller, T., Hüppi, R., Leifeld, J., 2019. Relationship between greenhouse gas emissions and changes in soil gas diffusivity in a field experiment with biochar and lime. J. Plant Nutr. Soil Sci. *182*, 667–675.

Kløve, B., Berglund, K., Berglund, Ö., Weldon, S., Maljanen, M., 2017. Future options for cultivated Nordic peat soils: Can land management and rewetting control greenhouse gas emissions? Environ. Sci. Policy *69*, 85–93.

Kløve, B., Sveistrup, T.E., Hauge, A., 2010. Leaching of nutrients and emission of greenhouse gases from peatland cultivation at Bodin, Northern Norway. Geoderma 154 (3–4), 219–232.

Koch, J., Elsgaard, L., Greve, M.H., Gyldenkærne, S., Hermansen, C., Levin, G., Stisen, S., 2023. Water table driven greenhouse gas emission estimate guides peatland restoration at national scale. Biogeosciences Discuss. 2023, 1–28.

Kroon, P.S., Schrier-Uijl, A.P., Hensen, A., Veenendaal, E.M., Jonker, H.J.J., 2010. Annual balances of CH4 and N2O from a managed fen meadow using eddy covariance flux measurements. Eur. J. Soil Sci. *61* (5), 773–784.

Leahy, S., Clark, H., Reisinger, A., 2020. Challenges and prospects for agricultural greenhouse gas mitigation pathways consistent with the Paris Agreement. Front Sustain Food Systv *4*, 69.

Leiber-Sauheitl, K., Fuß, R., Voigt, C., Freibauer, A., 2014. High CO2 fluxes from grassland on histic Gleysol along soil carbon and drainage gradients. Biogeosciences *11*, 749–761.

Leifeld, J., 2018. Distribution of nitrous oxide emissions from managed organic soils under different land uses estimated by the peat C/N ratio to improve national GHG inventories. Sci. Total Environ. 23–26, 631–632,.

Leifeld, J., Bassin, S., Fuhrer, J., 2005. Carbon stocks in Swiss agricultural soils predicted by land-use, soil characteristics, and altitude. Agric. Ecosyst. Environ. *105* (1–2), 255–266.

Leifeld, J., Menichetti, L., 2018. The underappreciated potential of peatlands in global climate change mitigation strategies. Nat. Commun. *9*, 1071.

Leppelt, T., Dechow, R., Gebbert, S., Freibauer, A., Lohila, A., Augustin, J., Drosler, M., Fiedler, S., Glatzel, S., Hoper, H., Jarveoja, J., Laerke, P.E., Maljamem, M., Mander, U., Makiranta, P., Minkkinen, K., Ojanen, P., Regina, K., Strömgren, M., 2014. Nitrous oxide emission hotspots from organic soils in Europe. Biogeosciences *11* (6), 9135–9182.

Linn, D.M., Doran, J.W., 1984. Effect of water-filled pore space on carbon dioxide and nitrous oxide production in tilled and nontilled soils. Soil Sci. Soc. Am. J. *48* (6), 1267–1272.

Mauder, M., Foken, T., 2006. Impact of post-field data processing on eddy covariance flux estimates and energy balance closure. Meteorol. Z. *15* (6), 597–610.

Merbold, L., Decock, C., Eugster, W., Fuchs, K., Wolf, B., Buchmann, N., 2021. Are there memory effects on greenhouse gas emissions (CO_2, N_2O and CH_4) following grassland restoration? Biogeosciences *18* (4), 1481–1498.

Moncrieff, J.B., Clement, R., Finnigan, J., Meyers, T., 2004. Averaging, detrending and filtering of eddy covariance time series. In: Lee, X., Massman, W.J., Law, B.E. (Eds.), Dordrecht Handbook of Micrometeorology: A Guide for Surface Flux Measurements. Kluwer Academic, pp. 7–31.

Moncrieff, J.B., Massheder, J.M., de Bruin, H., Elbers, J., Friborg, T., Heusinkveld, B., Kabat, P., Scott, S., Soegaard, H., Verhoef, A., 1997. A system to measure surface fluxes of momentum, sensible heat, water vapour and carbon dioxide. J. Hydrol. 188–189, 589–611.

Myhre, G., Shindell, D., Breon, F.-M., Collins, W., Fuglestvedt, J., Huang, J., Koch, D., Lamarque, J.-F., Lee, D., Mendoza, B., Nakajima, T., Robock, A., Stephens, G., Takemura, T., Zhang, H., 2013. Anthropogenic and natural radiative forcing. In: Stocker, T.F., Qin, D., Plattner, G.-K., Tignor, M., Allen, S.K., Boschung, J., Nauels, A., Xia, Y., Bex, V., Midgley, P.M. (Eds.), Climate Change 2013: The Physical Science Basis. Contribution of Working Group I to the Fifth Assessment Report of the Intergovernmental Panel on Climate Change. Cambridge University Press, Cambridge, UK.

Neftel, A., Blatter, A., Schmid, M., Lehmann, B., Tarakanov, S.V., 2000. An experimental determination of the scale length of N_2O in the soil of a grassland. J. Geophys Res *105*, 12095–12103.

Ochselin, S., Burgos, S., & Nussbaum, M. (2023). Bodenkartierung St. Galler Rheintal. Schlussbericht. ⟨https://www.bfh.ch/dam/jcr:fa2a317f-6a66-4c90-90fd-35094705b29e/BoKa_Rheintal_Schlussbericht_V1_compressed.pdf⟩ Accessed 04/10/2024.

Paul, S., Ammann, C., Alewell, C., Leifeld, J., 2021. Carbon budget response of an agriculturally used fen to different soil moisture conditions. Agric. Meteor. *300*, 108319.

Paul, S., Flessa, H., Veldkamp, E., López-Ulloa, M., 2008. Stabilization of recent soil carbon in the humid tropics following land use changes: evidence from aggregate fractionation and stable isotope analyses. Biogeochemistry *87*, 247–263.

Paul, S., Leifeld, J., 2023. Management of organic soils to reduce soil organic carbon losses. In: Rumpel, C. (Ed.), Understanding and Fostering Soil Carbon Sequestration. Burleigh Dodds Science Publishing, Cambridge, UK, pp. 617–680.

Peacock, M., Gauci, V., Baird, A.J., Burden, A., Chapman, P.J., Cumming, A., Evans, J.G., Grayson, R.P., Holden, J., Kaduk, J., Morrison, R., Page, S., Pan, G., Ridley, L.M., Williamson, J., Worrall, F., Evans, C.D., 2019. The full carbon balance of a rewetted cropland fen and a conservation-managed fen. Agric. Ecosyst. Environ. *269*, 1–12.

Poeplau, C., Jacobs, A., Don, A., Vos, C., Schneider, F., Wittnebel, M., Tiemeyer, B., Heidkamp, A., Prietz, R., Flessa, H., 2020. Stocks of organic carbon in German

agricultural soils—Key results of the first comprehensive inventory. J. Plant Nutr. Soil Sci. *183* (6), 665–681.
Poyda, A., Reinsch, T., Kluß, C., Loges, R., Taube, F., 2016. Greenhouse gas emissions from fen soils used for forage production in northern Germany. Biogeosciences 13 (18), 5221–5244.
Prévost, M., Plamondon, A.P., Belleau, P., 1999. Effects of drainage of a forested peatland on water quality and quantity. J. Hydrol. *214*, 130–143.
Reichstein, M., Falge, E., Baldocchi, D., Papale, D., Aubinet, M., Berbigier, P., Bernhofer, C., Buchmann, N., Gilmanov, T., Granier, A., Grunwald, T., Havrankova, K., Ilvesniemi, H., Janous, D., Knohl, A., Laurila, T., Lohila, A., Loustau, D., Matteucci, G., Valentini, R., 2005. On the separation of net ecosystem exchange into assimilation and ecosystem respiration: review and improved algorithm. Glob. Chang Biol. *11*, 1424–1439.
Säurich, A., Tiemeyer, B., Dettmann, U., Don, A., 2019. How do sand addition, soil moisture and nutrient status influence greenhouse gas fluxes from drained organic soils? Soil Biol. Biochem *135*, 71–84.
Schäfer, C.M., Elsgaard, L., Hoffmann, C.C., Petersen, S.O., 2012. Seasonal methane dynamics in three temperate grasslands on peat. Plant Soil 357, 339–353.
Schindler, U., & Müller, L. (1999). Rehabilitation of the soil quality of a degraded peat site. In D.E. Stott, R. H. Mohtar, & G. C. Steinhardt (Eds.), 2001.Sustaining the global farm. Selected papers from the 10th International Soil Conservation Organization Meeting held May 24–29, 1999 at Purdue University and the USDA-ARS National Soil Erosion Research Laboratory. <⟨https://topsoil.nserl.purdue.edu/nserlweb-old/isco99/pdf/iscodisc/Sustaining%20the%20Global%20Farm/P166-Schindler.pdf⟩> Accessed 04/10/2024.
Sognnes, L.S., Fystro, G., Øpstad, S.L., Arstein, A., Børresen, T., 2006. Effects of adding moraine soil or shell sand into peat soil on physical properties and grass yield in western Norway. Acta Agric. Scand., Sect. B - Soil Plant Sci. *56*, 161–170.
Soussana, J.F., Tallec, T., Blanfort, V., 2010. Mitigating the greenhouse gas balance of ruminant production systems through carbon sequestration in grasslands. Animal 4, 334–350. https://doi.org/10.1017/S1751731109990784.
Tiemeyer, B., Albiac Borraz, E., Augustin, J., Bechtold, M., Beetz, S., Beyer, C., Drösler, M., Ebli, M., Eickenscheidt, T., Fiedler, S., Förster, C., Freibauer, A., Giebels, M., Glatzel, S., Heinichen, J., Hoffmann, M., Höper, H., Jurasinski, G., Leiber-Sauheitl, K., Zeitz, J., 2016. High emissions of greenhouse gases from grasslands on peat and other organic soils. Glob. Chang Biol. *22*, 4134–4149.
Tiemeyer, B., Freibauer, A., Borraz, E.A., Augustin, J., Bechtold, M., Beetz, S., Beyer, C., Ebli, M., Eickenscheidt, T., Fiedler, S., Förster, C., Gensior, A., Giebels, M., Glatzel, S., Heinichen, J., Hoffmann, M., Höper, H., Jurasinski, G., Laggner, A., Drösler, M., 2020. A new methodology for organic soils in national greenhouse gas inventories: Data synthesis, derivation and application. Ecol. Indic. *109*, 105838.
Veenendaal, E.M., Kolle, O., Leffelaar, P.A., Schrier-Uijl, A.P., Van Huissteden, J., Van Walsem, J., Möller, F., Berendse, F., 2007. CO2 exchange and carbon balance in two grassland sites on eutrophic drained peat soils. Biogeosciences *4*, 1027–1040.
Velthof, G.L., & Rietra, R.P.J.J. (2018). Nitrous oxide emissions from agricultural soils. Wageningen, Wagening Environmental Research, Report 2921. <⟨https://library.wur.nl/WebQuery/wurpubs/fulltext/466362⟩> Accessed 04/10/2024.
Vickers, D., Mahrt, L., 1997. Quality control and flux sampling problems for tower and aircraft data. J. Atmos. Ocean. Technol. 14 (3), 512–526.
von Lützow, M., Kögel-Knabner, I., Ludwig, B., Matzner, E., Flessa, H., Ekschmitt, K., Guggenberger, G., Marschner, B., Kalbitz, K., 2008. Stabilization mechanisms of organic matter in four temperate soils: Development and application of a conceptual model. J. Plant Nutr. Soil Sci. *171* (1), 111–124.
Wall, A.M., Campbell, D.I., Mudge, P.L., Schipper, L.A., 2020. Temperate grazed grassland carbon balances for two adjacent paddocks determined separately from one eddy covariance system. Agric. Meteor. *287*, 107942.
Wang, Y., Paul, S.M., Jocher, M., Alewell, C., Leifeld, J., 2022. Reduced nitrous oxide emissions from drained temperate agricultural peatland after coverage with mineral soil. Front Environ. Sci. *157*.
Webb, E.K., Pearman, G.I., Leuning, R., 1980. Correction of flux measurements for density effects due to heat and water vapour transfer. Q. J. R. Meteorol. Soc. 106 (447), 85–100.
Weideveld, S.T.J., Liu, W., van den Berg, M., Lamers, L.P.M., Fritz, C., 2021. Conventional subsoil irrigation techniques do not lower carbon emissions from drained peat meadows. Biogeosciences *18* (12), 3881–3902.
Wilson, D., Blain, D., Couwenberg, J., Evans, C.D., Murdiyarso, D., Page, S.E., Renou-Wilson, F., Rieley, J.O., Sirin, A., Strack, M., Tuittila, E.-S., 2016. Greenhouse gas emission factors associated with rewetting of organic soils. Mires Peat *17*, Article 04.
Wüst-Galley, C., Heller, S., Ammann, C., Paul, S., Doetterl, S., Leifeld, J., 2023. Methane and nitrous oxide emissions from rice grown on organic soils in the temperate zone. Agric. Ecosyst. Environ. *356*, 108641.
Wutzler, T., Lucas-Moffat, A., Migliavacca, M., Knauer, J., Sickel, K., Šigut, L., Menzer, O., Reichstein, M., 2018. Basic and extensible post-processing of eddy covariance flux data with REddyProc. Biogeosciences *15*, 5015–5030.
Yu, Z., Loisel, J., Brosseau, D.P., Beilman, D.W., Hunt, S.J., 2010. Global peatland dynamics since the Last Glacial Maximum: Global Peatlands Since the LGM. Geophys. Res. Lett. *37*.
Zakharova, O.A., Musaev, F.A., Kucher, D.E., Vinogradov, D.V., Ushakov, R.N., 2020. Sanding of drained peatlands. BIO Web Conf. *17*, 00089.